

CAUSES OF DEFECTS IN HISTORICAL CERAMIC MATERIALS WITH Ca-RICH BODY

#PAVLA DVOŘÁKOVÁ*, ALEXANDRA KLOUŽKOVÁ*, MÁRIA KOLÁŘOVÁ*, MARTINA KOHOUTKOVÁ**

*Department of Glass and Ceramics, University of Chemistry and Technology Prague,
Technická 5, 166 28 Prague, Czech Republic

**Central Laboratories, University of Chemistry and Technology Prague,
Technická 5, 166 28 Prague, Czech Republic

#E-mail: pavla.dvorakova@vscht.cz

Submitted July 24, 2023; accepted August 31, 2023

Keywords: Glaze defects, Archaeological ceramics, Faience, X-ray methods, Stress states

The aim of the present work was to study and identify the causes and sources of defects in the glazes and decorations of archaeological ceramics containing a calcium component. As part of systematic archaeological research in the Hradčany area, several reconstructable objects and some fragmentary sherds of archaeological ceramics with a relatively high calcium content were found. Seven objects of faience were rescued from the waste pits on the premises of the third courtyard of the Prague Castle, a flower pot was found in Lumbe garden, and creamware sherds were excavated from a waste pit between the Salm and Schwarzenberg palaces on Hradčany Square. The first step of the research was the evaluation of ceramic bodies, glazes, and decorations using archaeometric methods. Subsequently, dilatometric measurements of ceramic bodies and stress state calculations of ceramic body-glaze, or glaze-decor systems were used to identify the sources of defects observed on archaeological finds. Both primary and secondary defects were identified in all studied finds. Among the primary defects, pinholes and blisters predominated. As secondary defects, crazing, blackening, corrosion, delayed peeling, and mechanical abrasion were recognised. Thanks to the combination of X-ray and optical methods, together with the determination of the stress states of the two- and three-component systems, causes of secondary defects were described. The main source of these defects were calcium residues causing volume changes in the ceramic bodies.

INTRODUCTION

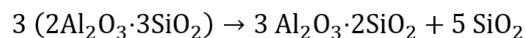
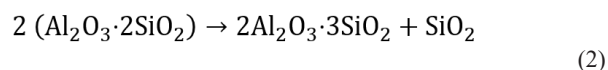
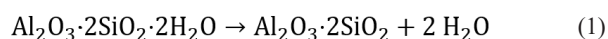
A typical representative of historical ceramic material with a calcareous ceramic body is faience, which belongs to the group of fine utilitarian ceramics with tin-lead glaze and onglaze decor.

The first faience originates from Mesopotamia and Persia from 4000 BC, but the frequently used term Egyptian faience did not appear until the 19th century. This is what European archaeologists called the ceramics produced in ancient Egypt. However, from the material and production technology point of view, it was not a real faience. The production consisted of mixing ground desert sand enriched in calcium, soda, and other alkaline and earth alkaline admixtures into a starting material that was shaped by hand or in moulds and then fired at a temperature of approximately 900 °C. The bright turquoise glaze contained the first artificially made pigment, the shade of the colour of which was determined by the composition and preparation conditions. The pigment was applied in a mixture with a flux containing natural evaporite, which was also used in the production of glass [1-4]. It has been indicated the use of different plant ashes for production of faience

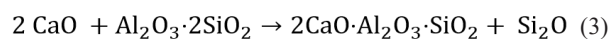
and glass-making, respectively [3,5]. Glazed ware with colourful decor came to Europe in the 14th century from the Middle East region, where it was used approximately from the 9th century onwards. A significant increase in imports occurred during the Renaissance and the name used – majolica was derived from the export ports in Mallorca [6]. European production is associated with the names of Bernard Palissy, Henry Deux, and especially with three generations of the della Robbia family [7]. The development of decors went in two directions, Urbino decors were associated with strong colour shades and with colours for high temperature decorations. The use of a milky bright glaze and a calcareous component in the ceramic body has been associated with the Italian city of Faenza since the second half of the 16th century. That is why the products were called faience in France and Germany. Central European producers, including the Moravian Habans, followed up on this type of ceramics with their production. The Urbino style was adopted by workshops in France and Germany, especially in the areas of Hamburg and Nuremberg. In the 18th century, Italian production lost its regional character and tried to get as close as possible to porcelain [6,8,9].

Until now, the term faience has traditionally been used for ceramic objects made from floated clays, quartz sand, and limestone. The surface is covered by a white tin-lead glaze with a coloured onglaze or in-glaze decor, often combined with plastic decoration [6,10,11]. For faience, the application of decoration on raw unfired glaze was typical (and still is). This glaze is applied after the first firing, which takes place at a higher temperature than the final firing. The range of colours was thus significantly limited. That is why muffle colours with a lower firing temperature started to be used. Currently, the firing temperature of a ceramic body with a calcareous component is reported to be in the range of 1000 – 1250 °C in order to obtain the desired properties [12,13]. The firing time ranges from about 40 minutes for porous objects and 60 to 70 minutes for sintered tiles [12,14-16]. During the firing of a calcareous ceramic body containing clay raw materials, two basic processes take place:

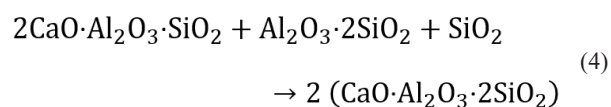
a. dehydroxylation of clay minerals (depending on the clay type approximately 500 °C) with subsequent mullite phase formation (from approx. 1000 °C); in the case of kaolinite with the formation of metakaolinite



b. decomposition of calcite (approx. 620 – 850 °C, depending on firing conditions and particle size) and subsequent reaction of products, i.e. reactive calcium oxide with metakaolinite to gehlenite



Gehlenite is a thermodynamically metastable phase that subsequently reacts to a stable anorthite:



The anorthite in a calcareous ceramic body has a fundamental influence on the resulting properties of the product, especially on strength and shrinkage. Its formation is determined by the mutual ratio of CaO, Al₂O₃, and SiO₂, which can be expressed using a ternary diagram (Figure 1). If a magnesium component is present, other crystalline phases such as diopside can form.

The course of firing, accompanied by the decomposition of the calcareous raw material and the subsequent reaction of the unstable phases into the stable ones, has a fundamental influence on the quality of faience decorations. If the firing is not conducted

correctly and CaO remains in the fired ceramic body, calcite recrystallisation occurs during usage. In the case of the presence of metaclays, their rehydroxylation also occurs [18,19]. Both processes are accompanied by the expansion of the ceramic body, which can be the source of secondary defects of glazed faience surfaces.

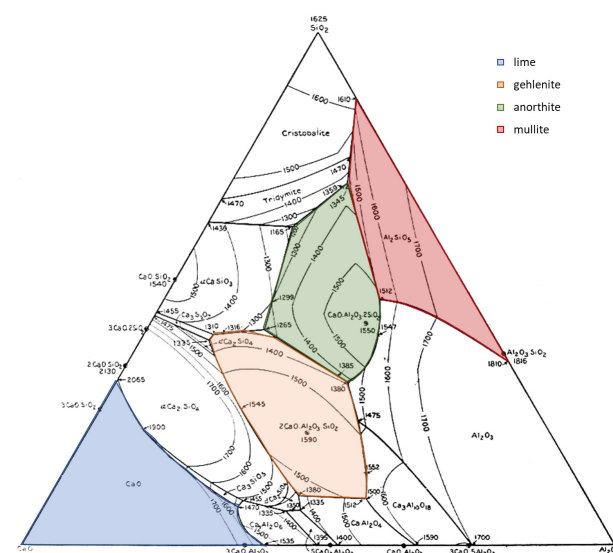


Figure 1. Ternary phase diagram in SiO₂-Al₂O₃-CaO [17].

Ceramic objects with a Ca component sometimes show primary defects, which arise mainly from:

- mismatch of thermal expansion coefficients of the decor/glaze/ceramic body,
- insufficient degassing of the ceramic body during the first firing, when pinholes and possibly blisters occur on the surface of the glaze or decor during the second firing,
- incorrect production technology – inappropriate density of the glaze slurry, wrong application of the glaze, the unclean surface of the fired ceramic body, unsuitable firing conditions, dust in the kiln, etc. can result in specking.

When assessing the defects of the glazed historical faience, it is necessary to consider both primary defects (given, for example, by unfamiliarity with the relatively demanding production technology at that time or failure of a worker or equipment), and secondary defects during usage. In the case of archaeological finds, another significant aspect had to be considered, namely the conditions of storage in the ground, e.g. in waste pits (pH, temperature, humidity, impurities, bacteria, etc.). During the research of the set of archaeological finds from Prague, four possible types of degradation of archaeological glazed ceramics were determined [20]. These degradation processes occurring in the ceramic body-glaze system are shown schematically in Figure 2.

Two types of primary defects – peeling of the glaze layer and crazing – are a result of the incompatibility of the glaze and the ceramic body. Degradation process (a) – i.e. the formation and growth of defects is then associated with the release of excessive stress in the ceramic body-glaze system already during cooling from the firing temperature. Other degradation processes (b, c, d) lead to the formation of secondary defects. Delayed crazing occurs due to moisture when secondary tensile stress is created in the glaze (b) by the moisture expansion of the ceramic body. This type of defect develops during the use of the object or during its subsequent deposition in the ground. It is caused by the processes taking place in the ceramic body (rehydration and rehydroxylation). Additional compressive stress in the glaze layer (c) causes secondary peeling of a glaze often called “delayed” peeling or bitty glaze. The reason may be an imperfectly prepared substrate with an uneven surface and large grains of quartz or other tempers at the interface with the glaze. The tension at the grain boundaries leads to an increase in the compressive stress in the glaze. If the glaze peels off the ware on edges of contours to relieve the stress, it is also called shivering. Another reason for the disrupted coherence of the system can be the migration of soluble salts through a ceramic body

with high porosity (typical for Ca-rich sherds) and a high content of unstable noncrystalline phases associated with expansion pressures due to weather conditions. As the roughness of the surface increases, the amount of surface defects increases, and the strength of the glaze decreases. Exceeding the strength failure limit of the glaze associated with its peeling can also lead to the deposition of products of surface corrosion or biocorrosion, or even to the growth of corrosion crusts under the glaze. In the case of biocorrosion, anaerobic sulfate-reducing bacteria (SRB) causes the so-called blackening, when black sulfides, e.g. lead sulfide, form on the glaze surface. These are manifestations of corrosion of the glaze itself without the influence of the ceramic body. The most common corrosion defects are efflorescence, iridescence, and growth and the presence of corrosion products. The combination of stress states together with the corrosive effect of the surrounding environment is included in the last part of the diagram (d). The effect of both processes simultaneously negatively influences the original equilibrium of the ceramic body-glaze system. The formation and growth of corrosion products, which preferentially precipitate in places of reduced cohesion and deteriorated surfaces, also contribute to the acceleration of the defect formation [20].

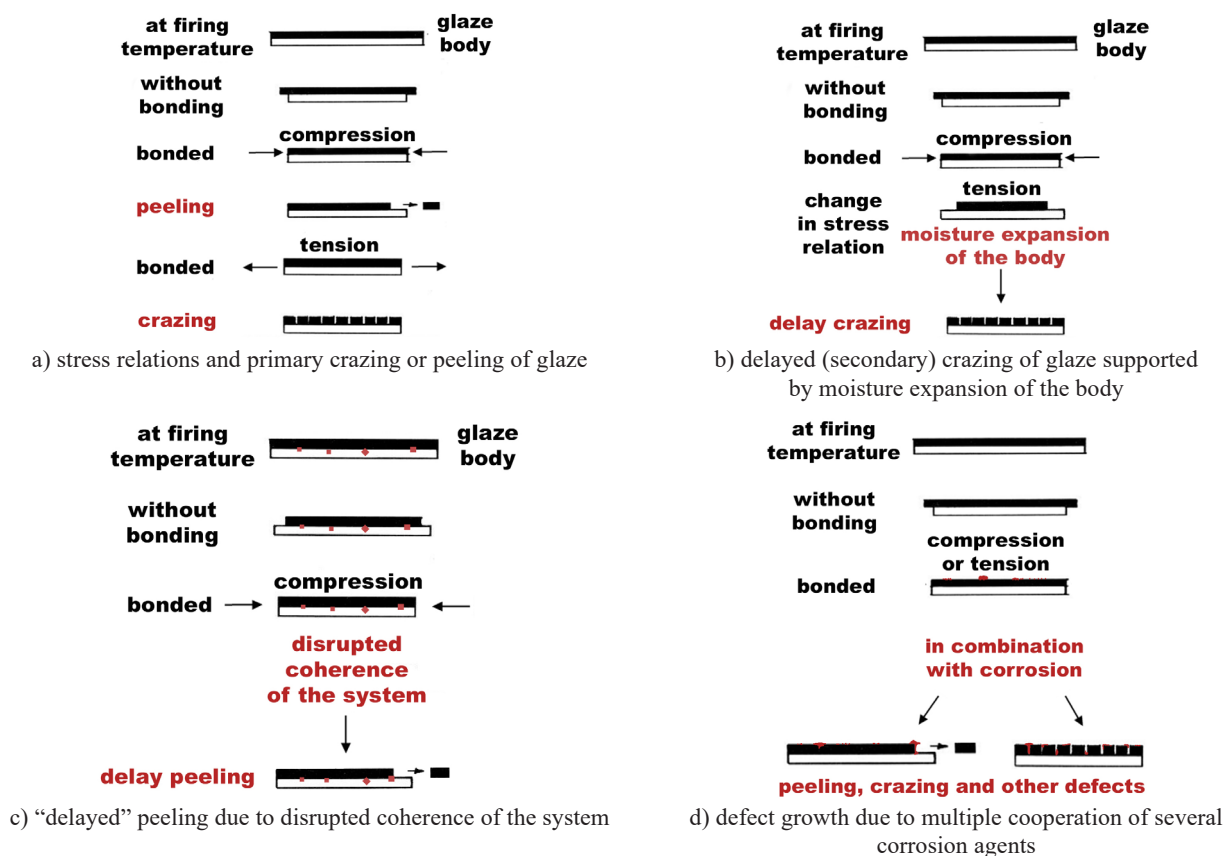


Figure 2. A scheme of possible degradation processes and the growth of defects growth [20].

In the case of glazed ceramics with onglaze decor (faience), it is necessary to evaluate the stress states of both interfaces, i.e. ceramic body-glaze and glaze-decor, in order to assess the causes of defects.

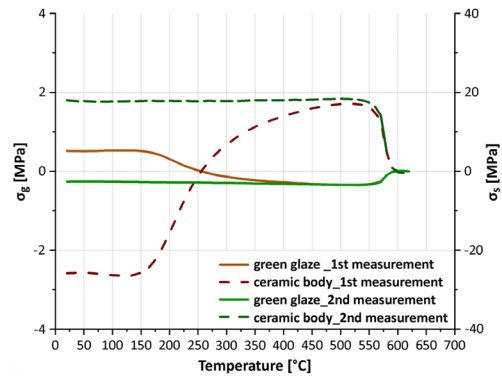
The evaluation of stress relations and the determination of thermal expansion coefficients (CTEs) could be carried out using several methods and devices [21,22]. The Steger test as the most accurate method of stress evaluation is capable of interpreting the development, character and magnitude of stress in the interlayer of a ceramic system [20,23-26]. The complicated preparation of the samples is the main disadvantage of this method. The specific shape of the sample is a difficult requirement to fit for most modern ceramics and is completely beyond practical possibilities for historical ceramic products. The stress relations within the ceramic body-glaze system can also be determined by dilatometry and thermomechanical analysis. The fairly accurate method of determining the stress relations, which is widely used in production, is the graphical comparison of the measured curves; the more precise method is to calculate the stresses using the equations [27-29]:

$$\sigma_g = \frac{(\alpha_s - \alpha_g)}{\frac{1 - \mu_g}{E_g} + \frac{1 - \mu_s}{E_s}} \times \frac{h_g}{h_s} \times \Delta T \quad (5)$$

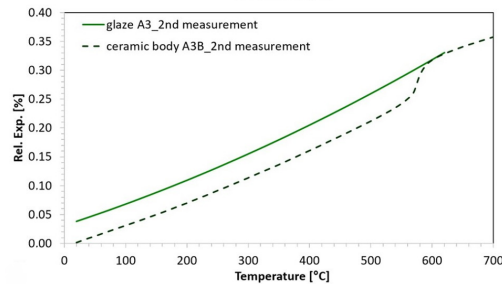
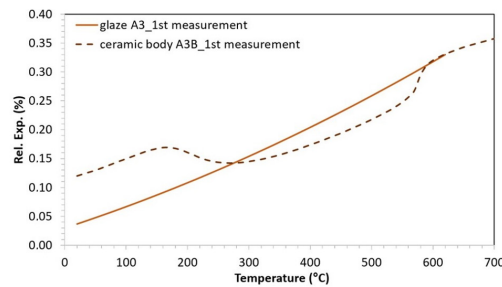
$$\sigma_s = \frac{(\alpha_s - \alpha_g)}{\frac{1 - \mu_g}{E_s} + \frac{1 - \mu_g}{E_g}} \times \frac{h_s}{h_g} \times \Delta T \quad (6)$$

where σ_g and σ_s are the stresses developed in the ceramic body/the glaze layer in MPa, α_s and α_g are the thermal expansion coefficients of the ceramic body and the glaze in K^{-1} , ΔT is the difference between the set point T_n (a temperature at which permanent mechanical stresses occur during cooling) and the ambient temperature T , μ_s and μ_g are the Poisson ratios of the ceramic body and the glaze, E_s and E_g are Young's moduli of the ceramic body and the glaze in MPa and h_s and h_g are thicknesses of the ceramic body or the glaze layer in μm . A positive absolute value of stress means that tensile stress is developed within the layer; on the contrary, a negative value corresponds to compressive stress developed. The graphical representation of the calculated stress values can effectively show the overall stress which is called the total mismatch of the system (Figure 3a). The dilatation measurement of samples of naturally aged finds (first measurement) includes the simultaneous effects of the CTE difference in the ceramic body-glaze system, when there is tensile stress in the glaze (solid brown curve), and dehydroxylation of the rehydroxylated component in the ceramic body (dashed brown curve), see Figure 3b. The second measurement of the same sample (Figure 3b, green curves) shows the effect of the difference in CTE when there is compressive stress in the glaze (solid green curve) and tensile stress in the ceramic body (dashed green curve).

This is the state of the product after the final firing. The graph documents the possibility of positive compressive stress in the glaze changing to disadvantageous tensile stress during the aging of the sherd material (during usage, in a waste pit, etc.). This process is typical for materials that contain residues of clay minerals (metaclays). The maximum effect of the moisture expansion of the ceramic body can be obtained by laboratory hydrothermal loading (artificially accelerated aging) and is part of the stability predictions in the ceramic body-glaze system of current products. When evaluating the stress states of two-component systems using dilatometric data, it is necessary to consider the total mismatch Δ (total stress difference). This term expresses the final stress difference for the system studied expressed from the absolute stress values σ of both components, in this case, it is 26.4 MPa for the first measurement and 18.3 MPa for the second [30,31].



a) calculated stress relations from the 1st and 2nd dilatometric measurement



b) graphical comparison of the measured curve of a ceramic body and the calculated curve of a glaze from the set point (T_n) to the ambient temperature

Figure 3. Example of graphic expression of stress relations and dilatometric measurements of the glazed tile system [31].

This paper is focused on the identification of defects sources in glazed archaeological finds with calcareous ceramic bodies. During the archaeological investigations of waste pits in the grounds of the Prague Castle [32] and the surrounding area, fragmentary material of blue-painted faience, a monochrome plate, a flower pot, and other colourfully decorated sherds, were found. The surfaces showed various defects and especially in the case of luxury faience, it was a question whether they came from production or were caused during use or when were stored in a waste pit. The methods used to predict the stability of glazes in contemporary glazed products were used for this evaluation. The initial step was a material survey of ceramic bodies, glazes, and decorations, using archaeometric methods.

Some objects were provided with a distinguishable mark, e.g. the faience small cup No. 5 and the faience saucer No. 4 with a pattern of pomegranates. Here it was possible to specify the period of production based on the manufacturer's signature BK (Figure 4). This signature proves the production of the finds in the Bayreuth manufactory in the years 1728 – 1744 [34], during the ownership period of Johann George Knöller (1678 – 1739). Three vessels were assigned to another German provenance, the Nuremberg area (possibly Ansbach, Hanau, etc.): plate No. 1, shallow bowl No. 2, and small cup No. 3 [32].

EXPERIMENTAL

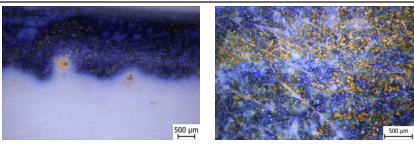
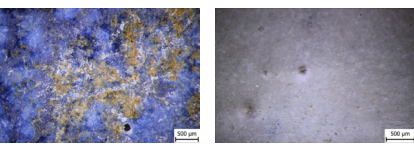
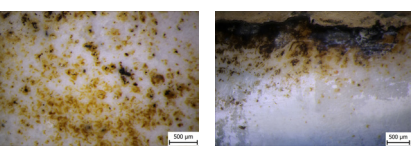
Materials

Ten restored objects were selected for the evaluation of defects, eight blue-decorated luxury faience finds (Nos. 1–8), a creamware plate with white glaze (No. 9), a flower pot with turquoise glaze (No. 12), and two calcareous sherds with blue decor and colourful painting (Nos. 10 and 11). For all evaluated artefacts, a description, dating, location of the site of finding, term of archaeological rescue, and a photodocumentations of the object including the observed defect, are given in Table 1 [33].



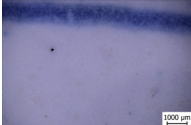
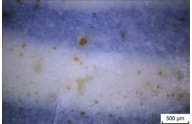
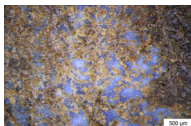
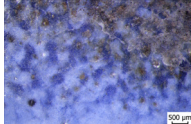
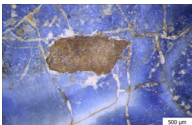
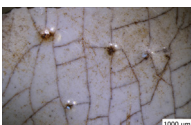
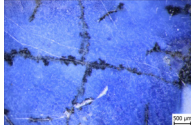
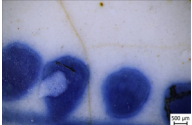
Figure 4. Detail of the faience mark on the saucer No. 4.

Table 1. Studied archaeological finds.

No.	name inventory number location term of archaeological rescue dating	Photodocumentation of the object after restoration	Photodocumentation of the surface including observed defects
1	faience-plate inv. no. 275 Prague Castle, third courtyard, waste pit C 1925 1700 – 1800		 pinholes mechanical abrasion, blackening
2	faience-shallow bowl inv. no. 282 Prague Castle, third courtyard, waste pit C 1925 1700 – 1800		 pinholes, blistering mechanical abrasion, blackening
3	faience-shallow cup inv. no. 282 Prague Castle, third courtyard, waste pit C 1925 1700 – 1800		 blistering, speckling mechanical abrasion, blackening

continued

Table 1. Studied archaeological finds. *continued*

4	faience-saucer inv. no. 587 Prague Castle, waste pit H 1929 1700 – 1800		 	speckling, shivering mechanical abrasion
5	faience-small cup inv. no. 591 Prague Castle, waste pit H 1929 1700 – 1800		 	speckling, beginnings of surface corrosion mechanical abrasion
6	faience-small cup inv. no. 600 Prague Castle, waste pit H 1929 1700 – 1800		 	blistering, shivering mechanical abrasion, blackening
7	faience-small mug inv. no. 608 Prague Castle, waste pit H 1929 1700 – 1800		 	pinholes, blistering, crazing of the blue decoration layer, shivering mechanical abrasion, “delayed” peeling, blackening, beginnings of surface corrosion
8	faience-small mug inv. no. 588 Prague Castle, waste pit H 1929 1700 – 1800		 	pinholes, blistering, crazing of the blue decoration layer mechanical abrasion, “delayed” peeling, efflorescence of the white glaze
9	creamware-plate inv. no. 303 Prague Castle, third courtyard, waste pit C 1925 1700 – 1825		 	pinholes, crazing, shivering mechanical abrasion beginnings of surface corrosion
10	fragment of creamware inv. no. 713 Salm Palace, 186/IV Hradčany Square 2009 – 2010 1800 – 1900		 	pinholes, rarely speckling, crazing mechanical abrasion, blackening, corrosion
11	fragment of creamware inv. no. 343 Salm Palace, 186/IV Hradčany Square 2009 – 2010 1800 – 1900		 	speckling within white glaze, rarely small pinholes within all coloured layers, crazing mechanical abrasion, beginning of corrosion – efflorescence of brown and yellow decoration layers
12	flower pot inv. no. 308 Prague Castle, Lumbe garden 2018 – 2019 1850 – 1920		 	rarely blistering mechanical abrasion

Methods

The following methods and devices were used to evaluate ceramic bodies and glazes:

- Optical microscopy – defects and homogeneity of glazes were observed in reflected light (RL) using an Olympus SZX9 stereomicroscope (Olympus Europa Holding, Germany) with a Canon EOS 1100D digital camera. To create fully sharp images, images with different levels of sharpness were composited using the DeepFocus module in the QuickPhoto Industrial 4.0 software. Further observation of glaze layers and decors was performed on thin-sections of samples taken perpendicular to the surface of the sherd, using an Olympus BX60 polarising microscope (Olympus Europa Holding, Germany) in parallel polarised light (PPL) and in crossed nicols (XPL). Images were taken using a Canon EOS 1100D digital SLR camera and evaluated using the QuickPhoto Industrial 4.0 software [33,35].

- Weighing samples in water (Archimedes' method) - determining the parameters of the ceramic bodies – water absorption E (%), bulk density OH ($\text{g}\cdot\text{cm}^{-3}$), apparent porosity P_{ap} (%), and apparent relative density d_{ap} ($\text{g}\cdot\text{cm}^{-3}$) [36].

- X-ray fluorescence (XRF) – the chemical composition of ceramic bodies (powder) and glazes (surface of compact samples) was measured using a fully automatic sequential wave-dispersive (WD) X-ray spectrometer PERFORM'X (Thermo ARL, Switzerland). The analysed powder samples of ceramic bodies were pressed into pre-pressed cups made of boric acid with a diameter of 40 mm and covered with 4 μm thick polypropylene foil (PP). For the measurement of surface layers and glazes, cleaned flat compact samples were selected. The spectrometer is equipped with an X-ray lamp with Rh anode type 4GN with a Beryllium window, a 4.2 kW generator, collimators, 6 crystals (AXBeB, AX03, PET, Ge111, LiF200, LiF220) and two detectors (proportional and scintillation). The samples were measured in a vacuum and evaluated using the semiquantitative standard-free software UniQuant 5, which is integrated into the Oxsas software. The statistical method of principal components (PCA, Principal Component Analysis) was used to show and classify the data set of the measured chemical composition of ceramic bodies and glazes [33,37].

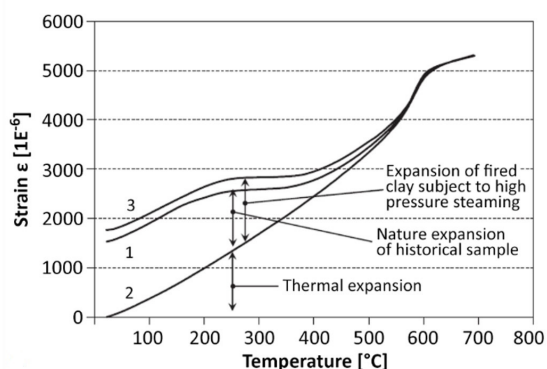
- Electron microscopy with chemical microanalysis (SEM/EDS) – the chemical composition of the selected samples was analysed using a TESCAN VEGA 3 LMU scanning electron microscope with an INCA 350 energy dispersive analyser in backscattered electron mode. The surface of the sample, prepared in the form of a cross-section, was coated with a 10 nm layer of Au in order to eliminate surface ionisation during observation at a higher resolution [38].

- X-ray diffraction (XRD) – the mineralogical composition was determined using a θ - θ powder diffractometer X'Pert³ Powder (PANalytical, Holland) with a parafocusing Bragg-Brentano geometry using $\text{CuK}\alpha$ radiation ($\lambda = 1.5418 \text{ \AA}$, $U = 40 \text{ kV}$, $I = 30 \text{ mA}$) in the angular range $5 - 80^\circ 2\theta$ at room temperature. Powder samples of ceramic bodies fine grounded in an agate bowl and flat compact samples of glazes were used for the measurements. Measured data were evaluated using the Panalytical High Score Plus 5.1 software. Semi-quantitative and quantitative phase analysis was performed using the Rietveld method and the PDF4⁺ database [33,37].

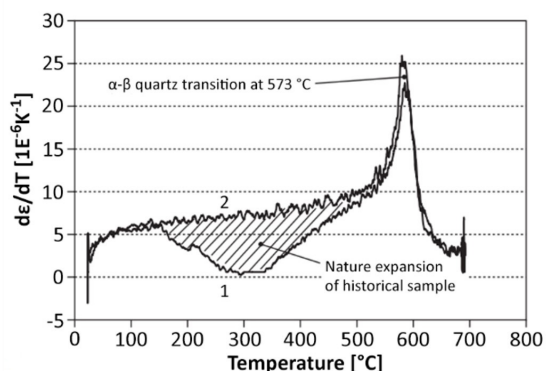
- Thermal analysis (DTA/STA) – monitoring of processes taking place during thermal loading of the sample (e.g., dehydration, dehydroxylation, decomposition reactions, melting, crystallisation, and transformation changes). Simultaneous thermal analyses in DTA-TG mode were performed using a LINSEIS STA Platinum Series 1600/1750 °C HiRes instrument (Linseis Messgeräte GmbH, Germany) with $50 \pm 0.05 \text{ mg}$ of a powder sample. Measurement was carried out in a platinum crucible with a lid at a heating rate of $10^\circ\text{C}\cdot\text{min}^{-1}$ from ambient temperature to temperatures of 1000 or 1200 °C. To ensure an inert atmosphere during the measurement, a controlled flow of helium or air ($15 \text{ ml}\cdot\text{min}^{-1}$) was used. The gases released during the measurement were analysed using a ThermoStarTM GSD320 (Pfeiffer Vacuum Technology AG, Germany) quadrupole-type mass spectrometer with a range of 300 AMU. The measurement was controlled by the Linseis Acquisition software, and the detection of released gases was performed using the Quedera 4.62 software. The measured data were processed in the Linseis TA Evaluation software [33,39,40].

- Dilatometry (DIL) - the study of the compatibility of the ceramic body-glaze system. A Linseis L75 HS 1600C PT dilatometer (Linseis Messgeräte GmbH, Germany) with a heating rate of $5^\circ\text{C}\cdot\text{min}^{-1}$ and a nominal force of 300 mN in a helium atmosphere in the temperature range of $25 - 700^\circ\text{C}$ was used to monitor the relative expansions and determine the thermal expansion coefficients ($CTEs$) of ceramic bodies. Piece samples of ceramic bodies in the form of compact prism samples measuring approx. $20 \times 5 \times 5 \text{ mm}$ were prepared for measurement. The measurement included several steps: the first measurement obtained the dependence of the strain of the sample on the temperature, which was influenced by the thermal expansion of the ceramic body, as well as by its contraction due to possible dehydroxylation. The second measurement of the same sample obtained a dependence corresponding only to the thermal expansion of the ceramic body. The selected samples (Nos. 1, 9, 12) were subsequently

subjected to hydrothermal treatment (HT) – load in an autoclave (230 °C, 2.77 MPa, 100 h) [41], followed by a third measurement documenting the maximum moisture expansion of the rehydroxylated sample in the autoclave, see Figure 5a.



a) dependence of strain on temperature



b) derivatives of the same dependence

Figure 5. An example of the dependence of strain on temperature of a historical clay ceramic sample – 1st measurement of the historical sample, 2nd measurement of the same sample and 3rd measurement of the sample after hydrothermal load measured by dilatometry [18].

In the case of glazes, it was not possible to take a sufficient amount of a sample for dilatometry or thermomechanical measurements, and therefore the characteristic temperatures and *CTE* values of the historical glazes were calculated using the SciGlass 6.7 software. Verification of the measured and calculated values of the coefficients of thermal expansion proved that for lead glazes, the calculated *CTE* values are slightly higher by approx. 8 %. This deviation and the error band, respectively, must be included in the calculations of the stress states of the historic ceramic body-glaze system [18, 19].

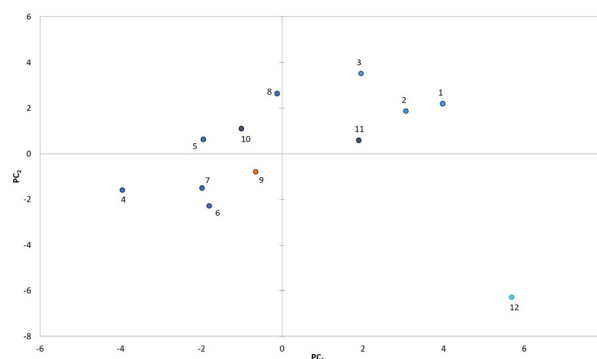
Calculations of stress relations were made from dilatometric measurements of the ceramic bodies and calculated *CTE* values of the glazes obtained using the software. Courses of stress states in the ceramic body-glaze system are presented in graphic form

and by indicating the value of the total mismatch Δ , which is used to express the total magnitude of the stress between the ceramic body and the glaze [31].

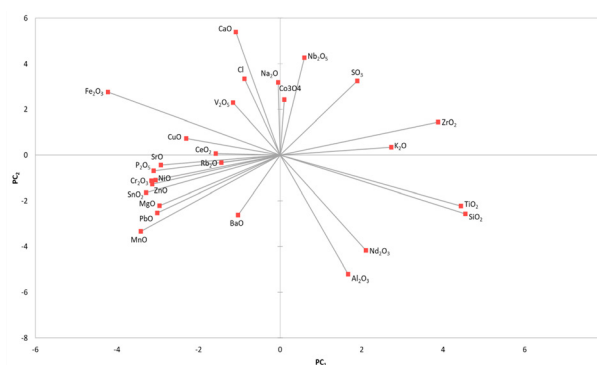
RESULTS AND DISCUSSION

Composition of ceramic bodies

The initial characterisation of glazes and ceramic bodies was carried out using X-ray methods (XRF, XRD) and by the determination of parameters of ceramic bodies. The processing of the XRF data in the form of a PCA diagram (Figure 6) confirmed the division of faience objects into two production area groups, to the finds from the Nuremberg area (Nos. 1 – 3) and from the Bayreuth manufactory (Nos. 4 – 8). The positions of the other points (Nos. 9 – 11) are between these groups and belong to separate fragments of calcareous sherds from the waste pit between Salm and Schwarzenberg palaces. The most different composition showed the youngest find – flower pot No. 12. All ceramic bodies were calcareous, and the CaO content of imported faience was in the range of 16 to 24 wt. %, white plate No. 9 contained 18 wt. % and turquoise flower pot No. 12 – 6 wt. % CaO. Another admixture of all ceramic bodies was the magnesium component in the range of 1.5 to 8 wt. % MgO.



a) PCA biplot of the chemical composition of Ca-rich ceramic bodies



b) biplot of active variables

Figure 6. Principal component analysis of studied ceramic bodies.

The mineralogical composition is presented in the form of a bar chart (Figure 7), from which it is evident that all the sherds contain stable crystalline phases created by the reaction of calcium and possibly magnesium components with metaclays during firing above 900 °C, i.e. mainly anorthite and diopside. Gehlenite was identified in the ceramic bodies of all samples except the flower pot No. 12. In some ceramic bodies, unreacted CaO remained after firing, which recrystallised into calcite during their deposition in the ground (samples Nos. 1 – 3, 9, 10, and 11). In the case of flower pot No. 12, there was probably a high content of clays in the raw material, and mullite and forsterite crystallised when fired above ~1000 °C (Figure 7). Diopside, forsterite, and other secondary minerals of the pyroxene group have been included into one group, called the pyroxene group.

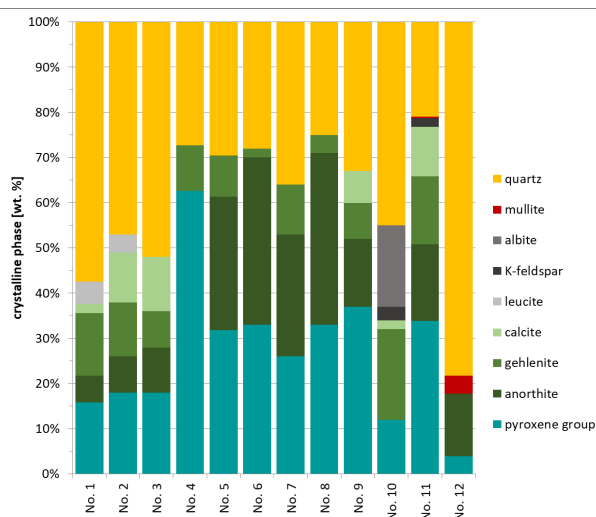


Figure 7. Mineralogical composition of samples with a calcium and magnesium component, bar chart.

The quantitative mineralogical composition was determined for samples Nos. 2, 5, 6, 9, 10, 11, and 12, using an internal standard method (Figure 8). The amount of amorphous phase ranged from 27 – 48 % in the case of faience; the most amorphous phase showed the sample of cup No. 6 - almost 50 %. The content of quartz ranged from 11 % to 24 %. The main attention was focused on the quantification of calcite and other Ca-containing minerals, e.g., in the bowl sample (No. 2) 4 % calcite, 16 % gehlenite, 4 % anorthite, 9 % minerals of the pyroxene group. Other minerals, e.g. 3 % leucite in sample No. 2, were also identified. Sample No. 5 showed a different composition from the other faience samples with a high content of minerals of the pyroxene group of about 57 % and 5 % gehlenite. It can be assumed according to the semi-quantitative XRD analysis (Figure 7) that in the case of sample No. 6, the content of pyroxenes will be even higher.

The sample of the white glazed plate No. 9 also showed a relatively high content of calcite (6 %); it also contained anorthite (15 %), gehlenite (4 %), and pyroxene group minerals (19 %). The amorphous phase covered about 1/3 of the ceramic body. The same amorphous phase content was identified in a single ceramic body with a mullite content (No. 12); the crystalline phase consisted of a high proportion of quartz (58 %), then mullite (5 %), anorthite (6 %), pyroxene group minerals (2 %) and traces of wollastonite. The creamware fragments showed high contents of the amorphous phase: fragments No. 10 (48 %) and No. 11 (38 %). Both samples contained calcium components in the form of calcite (6 – 7 %), gehlenite (8 – 11 %), anorthite (10 – 15 %), and pyroxene group minerals (7 – 10 %).

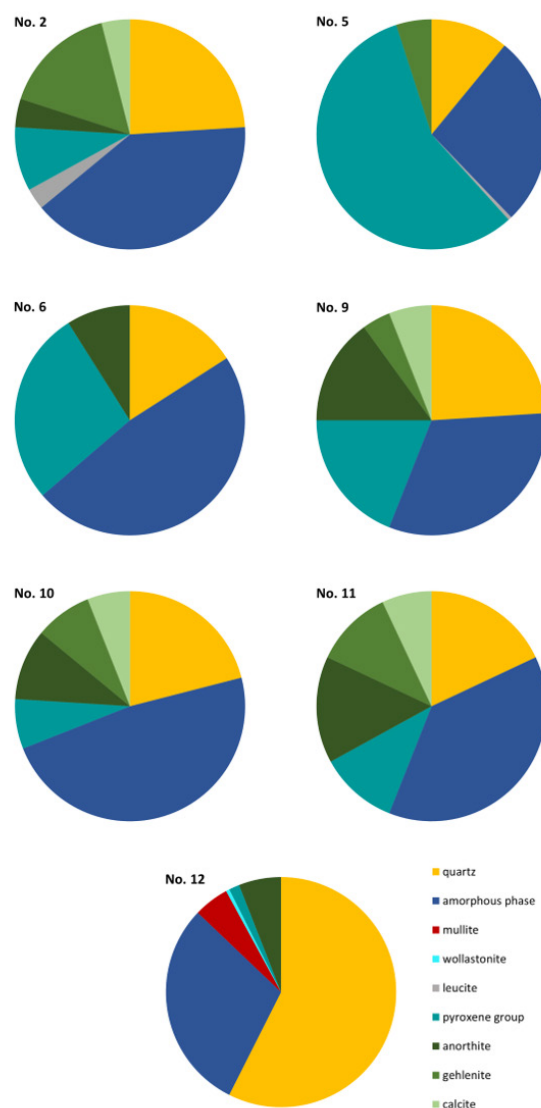


Figure 8. Mineralogical composition of selected samples with amorphous phase.

According to the type of ceramic body, relatively high values of water absorption and open apparent porosity were determined. For faience from the Nuremberg area, the values of water absorption were in the interval of 12 – 15 % and the open apparent porosity was 23 – 29 %. For the Bayreuth faience, the values were even higher, with water absorption in the range of 16 – 19 % and open apparent porosity of 25 – 36 %. These high porosity values led to the lightness and subtlety of these blue-and-white luxury objects, which in their appearance were close to the highly appreciated porcelain. For the other four samples, the values were in a wide interval – water absorption 13 – 25 % and open apparent porosity 23 – 38 %. The lowest values of water absorption (12 – 16 %) and open apparent porosity (25 – 30 %) showed plate No. 9 and a fragment of the plate with blue decor No. 10. Sample No. 12 (flower pot) showed high water absorption of approx. 18 % and apparent porosity of approx. 32 %. Fragment No. 11 had the highest values of water absorption of approx. 25 % and open apparent porosity of approx. 35 %.

Composition of glazes

All glazes are low to medium lead with contents of 15 – 44 wt. % PbO with an admixture of a calcium component in the range of 1 – 4 wt. %. White opaque glazes contain different amounts of SnO₂ as an opacifier, from 0.3 to 13 wt. %, depending on the type and colour of the glaze. For example, the white glaze of saucer No. 4 contains 13 wt. % PbO and 11 wt. % SnO₂; in the place of the blue decor 19 wt. % PbO, 11 wt. % SnO₂ and 0.7 wt. % Co₃O₄ was then identified. Cobalt ions are the most intense glass dye, 0.05 wt. % Co is enough to colour glass [42,43]. The presence of As, Ni, Bi, W, Mo, U, and Fe is also reported for cobalt ores from the Ore Mountains area, which had been used at least since the early Middle Ages [44]. Increased potassium content (4.7 wt. %, SEM/EDS) in the blue layers of the mug No. 8 (Figure 9) indicates the application of enamel, a cobalt glass frit [45]. This assumption is also confirmed by the combination of NiO-ZnO-Bi₂O₃ oxides (XRF) found in some blue decors, for example, in the shallow bowl No. 2, which is typical for enamels from the Ore Mountains [46]. There were production centres on both sides of the mountains, both on the Czech side, e.g. Soví hut', Horní Blatná, Potůčky, and on the German side, e.g. Johannegeorgenstadt, Schneeberg, from where enamel was probably imported to the Bayreuth and Nuremberg areas.

Degradation of glazes

Various types of defects were found on the surfaces of white glazes and cobalt decors (Table 2). Primary defects – especially pinholes (Figure 10), were observed to a large extent in the white-glazed plate (No. 9),

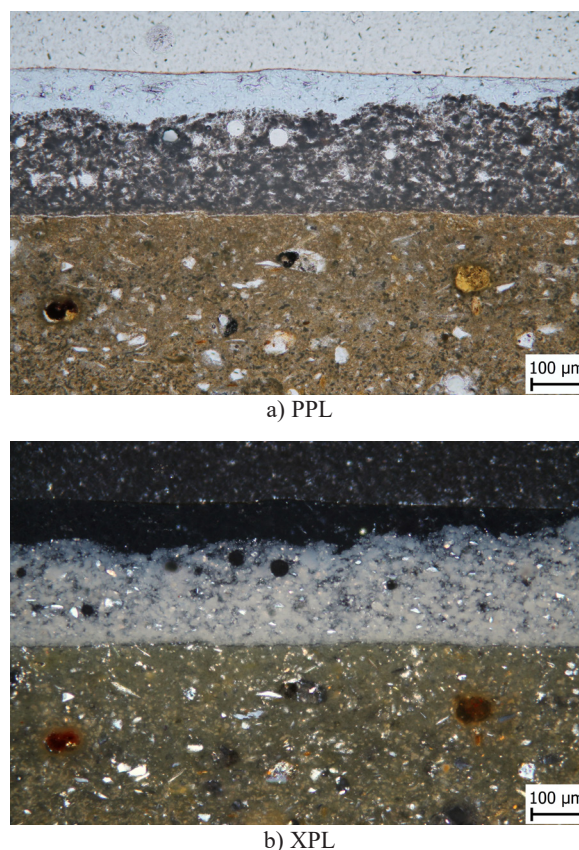


Figure 9. Thin-section of faience sample No. 8.

creamware sherds (Nos. 10 and 11), and rarely in the faience samples (Nos. 1, 7, 8). These defects originate from firing as a consequence of incomplete degassing (release of CO₂ during the decomposition of limestone) during the first firing. During the second firing with the glaze already applied, gases were additionally released when the glaze melted. Some bubbles reached the surface, where they created various pinholes. On other faience samples (Nos. 2, 3, 6, 7, and 8) and rarely on sample No. 12, blisters were observed. These are also primary defects when the glaze melts around the pinholes. Another very common primary defect – speckling, when the glaze is contaminated by the kiln atmosphere and black dots are formed on the surface, was uniquely identified on samples Nos. 2, 3, 4, 5, 8, and 11.

The surfaces of the faiences showed especially secondary defects caused by mechanical abrasion and the instability of the colouring components in the presence of a highly corrosive environment associated with biodegradation (Nos. 1, 2, 3, 5, 6, and 7). In addition to cassiterite, the presence of marcasite was also noted in the glazes of samples Nos. 1, 2, and 7. The formation of this mineral is associated with the biological deterioration of cobalt dyes by bacteria [47]. This type of defect in archaeological ceramics with high-lead glazes is also called as blackening (Figure 11). On some faience samples (Nos. 3, 5, and 6), surface corrosion of the white glaze was also observed.



a) PPL



b) XPL

Figure 10. Detail of thin-section of faience sample No. 7 – an orange arrow indicates the typical pinholing.

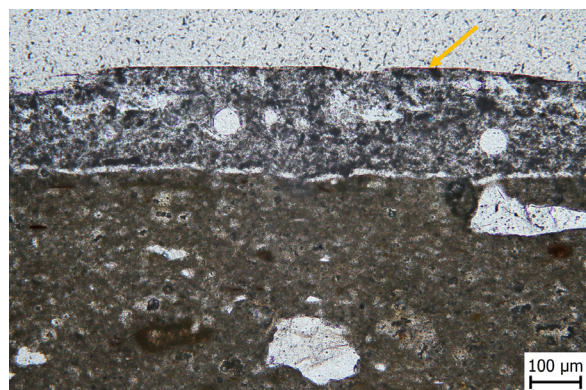


Figure 11. Detail of the thin-section of the faience sample No. 5 in PPL with blackening of the blue cobalt decoration layer.

Sample of mug No. 8 showed a relatively larger number of primary and secondary defects compared to the other samples of faience. A large number of cracks is visible on its surface, which have melted edges, especially in the case of the blue decor (Figure 2c and Table 1). It is obvious that the defects were already created during its production (Figure 12). Degassing of the large grains accompanied by the formation of large pores within the ceramic body caused the appearance of defects on the surface of the glaze. In some parts of these cracks, efflorescence containing mainly



Figure 12. A detail of the thin-section of sample No. 8 with a large pore around the Ca grain continues in the form of a crack to the surface.

chlorides, phosphates, and sulfates were identified. Some cracks were also observed on samples Nos. 9, 10, and 11, and dilatometric measurements including laboratory hydrothermal loading were used to determine the source of these defects.

The results of the dilatometric measurements are presented in graphic form in Figure 13. A comparison of the curves of relative expansions of glazes and ceramic bodies proved the conformity of the thermal expansion coefficients of both components. The second measurement, which characterise only the differences in the *CTE* of the glaze and the ceramic body, identified moderate compressive stress in the glaze layer for all samples. Therefore, the source of the observed cracks was not a bad choice of glazes, i.e. they were not primary defects from production, but secondary ones created afterward.

The first dilatation measurements showed that the use and subsequent storage of the fragments in the soil resulted in only a slight reduction in compressive stress within the glaze. The most significant decrease was found in samples Nos. 11, and 9 (Figure 13b). The blue band around the glaze curve represents the error band of the calculated *CTE* values of the lead glazes. It can be seen that the lower limit of this band at room temperature approaches the values of the second measurement of the ceramic body. It can be assumed that under further loading by external conditions could cause change of the stress in the glaze layer.

Specific stress values σ measured (for ceramic bodies) and calculated (for glazes) of these three samples Nos. 1, 9, and 12 are shown in Table 2. The total mismatch Δ values for the 1st, 2nd, and 3rd dilatation measurements were calculated from the stress relations of the ceramic bodies and glazes. The trend of dilatation curves described above is expressed here by the decrease in total mismatch values due to both usage and subsequent storage in the soil (2nd measurement) and due to hydrothermal load in the autoclave (3rd measurement).

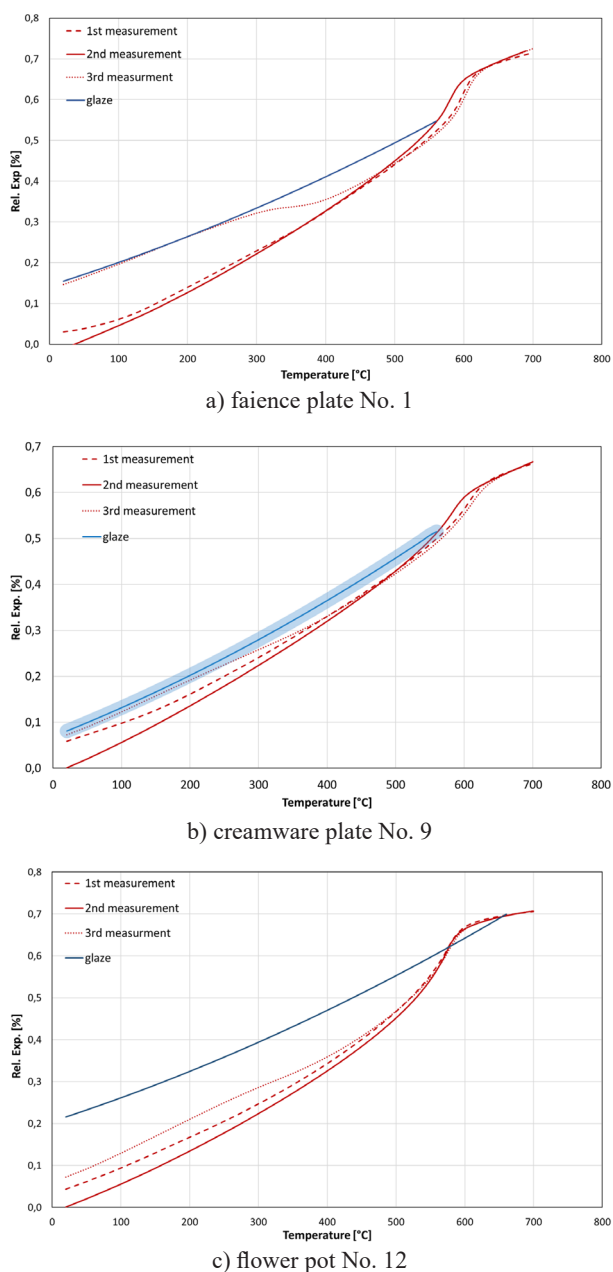


Figure 13. Calculated (glazes) and measured (ceramic bodies) relative expansion curves of the samples Nos. 1, 9, and 12.

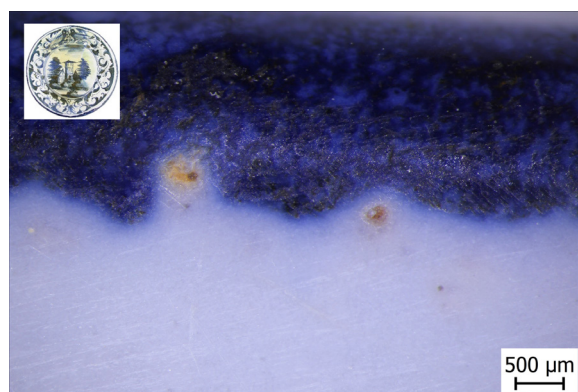
The stress between the ceramic body and the glaze (the total mismatch) for the evaluated faience samples reached a maximum value of 76.66 MPa (Table 2), which is below the limit leading to the formation of defects (100 MPa) [31]. In the case of onglaze decors, a three-component system has to be taken into account, where two combinations must be evaluated: ceramic body-glaze and glaze-decor. Both such systems were evaluated in the plate sample No. 4. In the first combination, the glaze was under compressive stress, whereas in the second combination, the glaze was under tensile stress and the blue decor was under compressive stress. Therefore, the plate surface did not show any defects associated with primary CTE mismatch or secondary expansion [20,33].

Figure 14 clearly shows the course of stress within the glaze layers and within the ceramic bodies of the respective samples. Faience is represented by the plate sample No. 1 (Figure 14b) and it is clear that the content of secondary calcium compounds formed during firing ensured minimal damage due to the effect of moisture expansion, as there are no residues of reactive clay minerals. In three samples Nos. 9, 10 and 11, the opposite problem occurred – the released CaO after the decomposition of calcite did not have metaclays available, so it did not react to another calcium silicate mineral during firing. Subsequently, under the influence of soil moisture, the free CaO hydrated and was the source of volume increase (up to 14 %) [48]. Recrystallisation of calcite takes place subsequently or simultaneously. The consequences can be similar to that of moisture expansion and lead to the formation of cracks, depending on the size and amount of grains and the thickness of the sherds.

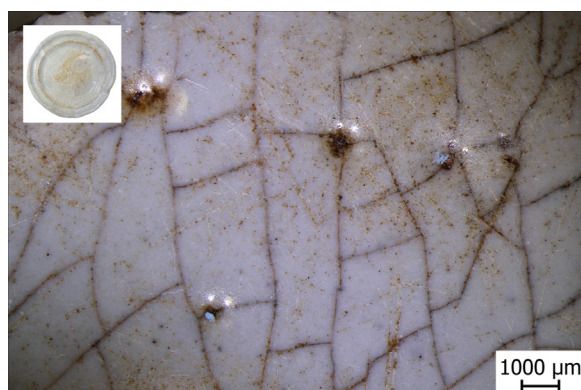
This most pronounced secondary defect was observed in the glaze of white plate No. 9 (Table 1, Figure 14c) containing 7 wt. % calcite and also in creamware sherds Nos. 10, and 11. In the other objects, this process was not so strong to cause such deterioration of surfaces. Pronounced primary defects (Figure 12 and Table 1) were proved in faience mug No. 8, which were subsequently attacked

Table 2. Stress σ developed within the glaze or ceramic body and total mismatch Δ of measured glaze-ceramic body systems in MPa.

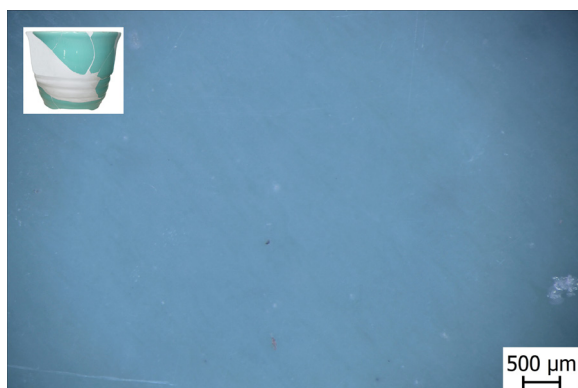
sample		developed stress within the layer σ			total mismatch Δ		
		2 nd measurement	1 st measurement	3 rd measurement (HT)	2 nd measurement	1 st measurement	3 rd measurement (HT)
1	body	61.35	45.41	27.45	63.80	47.23	28.55
	glaze	-2.45	-1.82	-1.10			
9	body	37.96	19.10	15.27	39.47	19.86	15.78
	glaze	-1.52	-0.76	-0.61			
12	body	73.71	56.80	46.31	76.66	59.07	48.16
	glaze	-2.95	-2.27	-1.85			



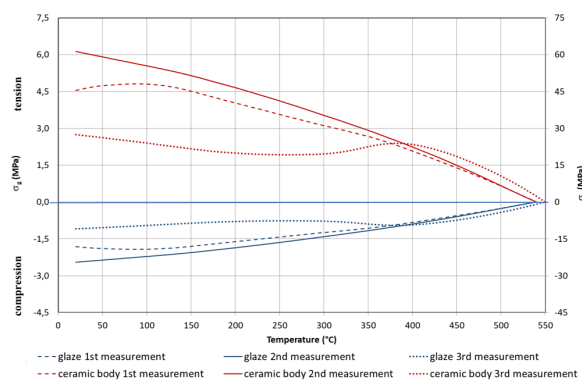
a) pinholes in glaze of the plate No. 1



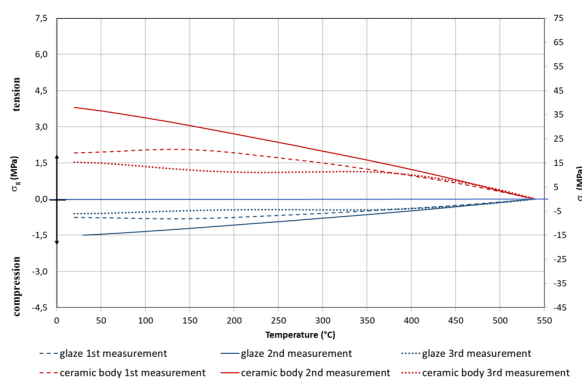
c) crazing and pinholing of the plate No. 9



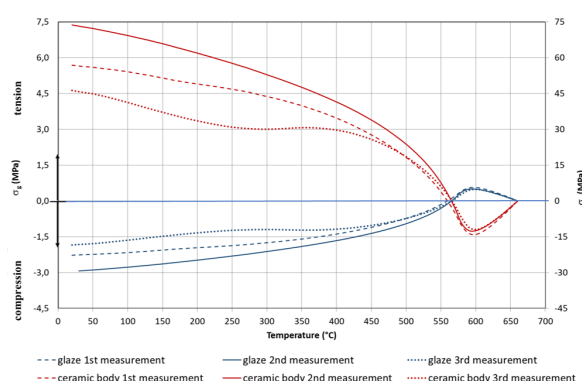
e) intact glaze of the flower pot No. 12



b) stress relation curves of the sample No. 1



d) stress relation curves of the sample No. 9



f) stress relation curves of the sample of flower pot No. 12

Figure 14. Stress relations of the ceramic body-glaze system of the samples Nos. 1, 9, and 12.

by corrosion and efflorescence formed here. Another interacting process was the water/ice transformation, which also created non-negligible crystallisation pressures.

In a third type of ceramic body (Figure 14e) containing mullite, volume expansion of the sherd under hydrothermal loading was identified, although very low. In this case, the expansion was caused by the rehydroxylation of the residues of the meta-clay component contained in the amorphous phase. The low content of the calcium component was not enough to react with all the residuals of clay minerals, and the hydrothermal load enabled moisture expansion of the ceramic

body. The source of the rearrangement of the stress curves (Figure 14f) was the volume change that accompanies the $\alpha \rightarrow \beta$ transformation of quartz at 573 °C.

Another secondary defect identified in faience samples Nos. 7, and 8 is also related to calcite recrystallisation – “delay” peeling. In the case of the plates (Nos. 4, and 9), shivering was observed (chipping of the glaze at the edges) due to a combination of three effects – of the curved surface, the presence of larger grains of temper mineral, and, above all, of the recrystallisation of carbonates under the surface of the glaze (Figure 15).

The effect of the curved edge of the object and the presence of grains just below the glaze can be seen in the thin section of the white glazed

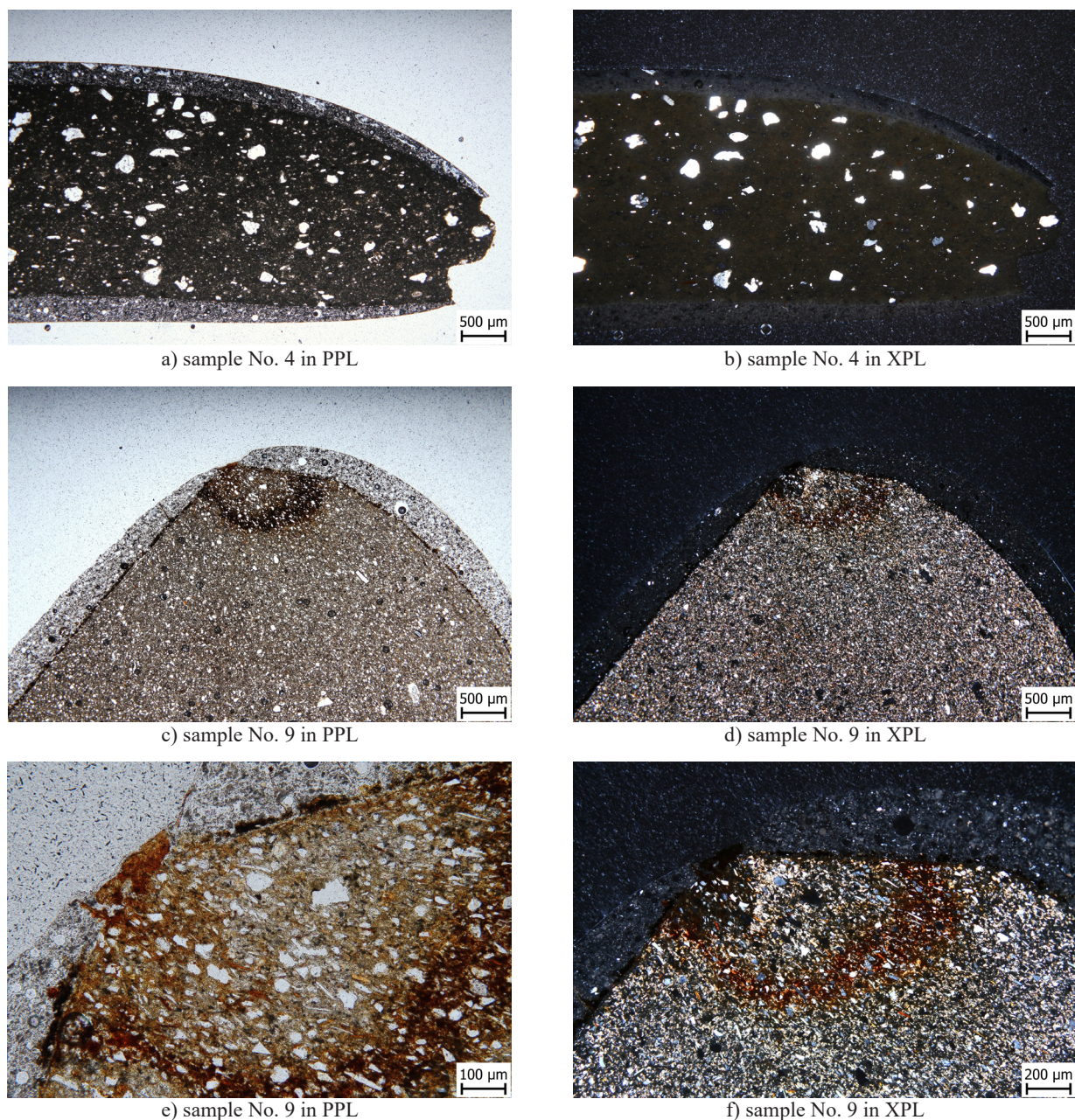


Figure 15. Thin-section of the samples Nos. 4 and 9, PPL on the left hand side, XPL on the right hand side.

plate sample (Figure 15a, b). Further on plate No. 9, a combination of primary defect pinholes created during the additional release of gasses during firing with glaze and the subsequent reaction of unreacted CaO back to calcite is documented in Figures 15c, d, e, and f. Recrystallisation led to the enlargement of the defect and the formation of cracks.

CONCLUSIONS

Defects of glazes and decorations of archaeological ceramics containing a calcareous component – faience lifted from waste pits in the premises of Prague Castle,

a flower pot from the Lumbe Garden, and ceramic finds from a waste pit between the Salm and Schwarzenberg Palaces were studied. The aim of the work was to identify the sources of defects observed on these archaeological finds, for which dilatometric measurements and calculations of the stress states of the systems ceramic body-glaze, or glaze-decor were mainly used. Detected defects can be divided into two groups:

- Primary defects – bubble defects (pinholes, blisters), specking, and shivering,
- Secondary defects – delayed crazing, mechanical abrasion, blackening, corrosion, delayed peeling.

Primary pinholes and blisters were identified mainly on the white plate (No. 9), the creamware (Nos. 10

and 11), and the faience mug (No. 8). On the other faience samples, the primary defects were rare. The source of these defects was insufficient degassing after calcite decomposition during the first firing.

Secondary crazing was again the most pronounced on the white glazed plate (No. 9), then on creamware sherds (No. 10, 11), and rarely on faience (No. 8). The causes of defects were identified using dilatation measurement, determination of calcareous minerals (gehlenite, anorthite, calcite, and pyroxenes) and optical microscopy observation. The incompatibility of CTE values in both systems (ceramic body-glaze, glaze-decor) as the cause of the defects was refuted. The fundamental source of these defects was the combination of stress due to the volume increase of calcium residues after the calcite decomposition and its subsequent recrystallisation due to the influence of the surrounding environment in the waste pit. Mechanical scratches created during the use of objects can be included in the group of secondary defects and were observed on all samples, including the very stable surface decoration of the flower pot.

REFERENCES

- Weiss G. (2007). *Keramika - umění z hlíny. Kulturní dějiny a keramické techniky*. 1st ed. Grada. ISBN 978-80-247-1954-2.
- Rehren T. (2008): A review of factors affecting the composition of early Egyptian glasses and faience: alkali and alkali earth oxides. *Journal of Archaeological Science*, 35(5), 1345–1354. doi: 10.1016/j.jas.2007.09.005
- Tite M.S., Manti P., Shortland A.J. (2007): A technological study of ancient faience from Egypt. *Journal of Archaeological Science*, 34(10), 1568–1583. doi: 10.1016/j.jas.2006.11.010
- Tite M.S., Shortland A., Maniatis Y., Kavoussanaki D., Harris S.A. (2006): The composition of the soda-rich and mixed alkali plant ashes used in the production of glass. *Journal of Archaeological Science*, 33(9), 1284–1292. doi: 10.1016/j.jas.2006.01.004
- Sparavigna A.C. (2012): Faience: the ceramic technology of ancient Egypt. *Archaeogate: Archeologia Sperimentale*, ISSN 1973-2953.
- Kybalová J. (1993). *Evropská Fajáns*. Uměleckoprůmyslové muzeum v Praze. ISBN 80-7101-013-8.
- Kotková O., Šefců R. (2022). *Sochy z hlíny: Terakoty italských mistrů 15.–19. století ze sbírek Národní galerie Praha*. Národní galerie Praha. ISBN 978-80-7035-806-1.
- Radványi D., Réti L. (2016). *Keramické umění Habánů*. Novella Könyvkiadó. 25. ISBN 978-963-9886-20-9.
- Sojka J. (2011). *Porcelán na Pražském hradě – Krása a užitek*. Správa Pražského hradu. 144–147. ISBN 978-80-86161-71-6.
- Hanykř V., Kutzendörfer J. (2008). *Technologie keramiky*. 2nd ed. Silikátový svaz. ISBN 80-903113-1-8.
- Maggetti M. (2012): Technology and Provenancing of French faience. *Archaeometry and Cultural Heritage: the Contribution of Mineralogy*. Madrid: Sociedad Española de Mineralogia. ISSN 1698-5478.
- Dvořáková P., Oujirí F., Kloužková A., Kolářová M., Kohoutková M. (2019): Influence of composition on properties of a calcium ceramic body, in: *Proceedings of the XIIIth International Conference Preparation of Ceramic Materials*. Technická univerzita v Košiciach, 153–157. ISBN 978-80-553-3314-4.
- Fiori C., Fabbri B., Donati G., Venturi I. (1989): Mineralogical Composition of the Clay Bodies Used in the Italian Tile Industry. *Applied Clay Science*, 4. doi: 10.1016/0169-1317(89)90023-9
- Svoboda L., Bažantová Z., Myška M., Novák J., Tobolka Z., Vávra R., Vimmrová A., Výborný J. (2018). *Stavební hmoty*. 4th ed. Luboš Svoboda. ISBN 978-80-260-4972-2.
- Hlaváč J. (1981). *Základy technologie silikátů*. 1st ed. Nakladatelství technické literatury.
- Dondi M., Raimondo M., Chiara Z. (2014): Clays and bodies for ceramic tiles: Reappraisal and technological classification. *Applied Clay Science*, 96, 91–109. doi: 10.1016/j.clay.2014.01.013
- Rankin G.A., Wricur F.E. (1915): The Ternary System CaO-Al₂O₃-SiO₂. *The American Journal of Science*, 229, 1–80. ISSN 0002-9599.
- Kloužková A., Kavanová M., Kohoutková M., Zemenová P., Dragoun Z. (2016): Identification of causes of degradation of Gothic ceramic tiles by thermal analyses. *Journal of Thermal Analysis and Calorimetry*, 125(3), 1311–1318. doi: 10.1007/s10973-016-5488-5
- Kavanová M., Kloužková A., Kloužek J. (2017): Characterization of the interaction between glazes and ceramic bodies. *Ceramics-Silikaty*, 61(3), 267–275. doi: 10.13168/cs.2017.0025
- Kolářová M., Kloužková A., Kohoutková M., Kloužek J., Dvořáková P. (2023): Degradation processes of medieval and renaissance glazed ceramics. *Materials*, 16(1), 375. doi: 10.3390/ma16010375
- Peterson M., Bernardin A.M., Kuhnen N.C., Riella H.G. (2007): Evaluation of the steger method in the determination of ceramic-glaze joining. *Journal of Material Science*, 466(1–2), 183–6. doi: 10.1016/j.msea.2007.02.046
- Schurecht H.G. (1943): Fitting glazes to ceramic bodies. *Journal of the American Ceramic Society*, 26(3), 93–8. doi: 10.1111/j.1151-2916.1943.tb15195.x
- Tandon R., Green D.J. (1990): Residual stress determination using strain gage measurements. *Journal of the American Ceramic Society*, 73(9), 2628–33. doi: 10.1111/j.1151-2916.1990.tb06738.x
- Blakely A.M. (1938): Life history of a glaze: II, measurement of stress in a cooling glaze. *Journal of the American Ceramic Society*, 21(7), 243–51. doi: 10.1111/j.1151-2916.1938.tb15772.x
- Johnson A.L. (1939): Stresses in porcelain glazes. *Journal of the American Ceramic Society*, 22(1–12), 363–6. doi: 10.1111/j.1151-2916.1939.tb19481.x
- Mattyasovszky-Zsolnay L.I. (1946): Delayed thermal contraction and crazing of ceramic glazes. *Journal of the American Ceramic Society*, 29(7), 200–3. doi: 10.1111/j.1151-2916.1946.tb11580.x
- Oujirí F. (2005): Napěťové vztahy v systému stěp-glazura granilie. *Zpravodaj Silikátového svazu*, 2, 10–20. ISSN 1210-2520.
- Plešingerová B., Klapáč M., Kovalčíková M. (2002): Moisture expansion of porous biscuit bodies-reason of

- glaze cracking. *Ceramics-Silikáty*, 46(4), 159–65. ISSN 1804-5847.
29. Kingery W.D. (1955): Factors affecting thermal stress resistance of ceramic materials. *Journal of the American Ceramic Society*, 38(1), 3–15. doi: 10.1111/j.1151-2916.1955.tb14545.x
 30. ČSN EN ISO 10545-10 (725110) (2022). Keramické obkladové prvky – Část 10: Stanovení změn rozměrů vlivem vlhkosti. Český normalizační institut.
 31. Kolářová M., Kloužková A., Kloužek J., Schwarz J. (2020): Thermal behaviour of glazed ceramic bodies. *Journal of Thermal Analysis and Calorimetry*, 142(1), 217–229. doi: 10.1007/s10973-020-09484-3
 32. Blažková G., Vepřeková J., (2015). *Nálezy hmotné kultury z renesančních odpadních jám z Pražského hradu. Material Finds from the Renaissance Waste Pits at Prague Castle*. Castrum Pragense 13, Archeologický ústav AV ČR, Praha, v. v. i., 533–553. ISBN 978-80-87365-85-4.
 33. Kloužková A., Kolářová M., Blažková G., Dvořáková P., Svobodová L., Kohoutková M., Žáček V., Adámek F., Zavřel J., Šefců R. (2022). *Příběh keramiky hradčanských paláců*. Vysoká škola chemicko-technologická v Praze (VŠCHT Praha). ISBN 978-80-7592-141-3.
 34. Hofmann F.H. (1928). *Geschichte der Bayreuther Fayencefabrik St. Georgen am See*. Augsburg, Benno Filser Verlag G. m. b. H.
 35. Přístrojové vybavení. [online]: <https://restauro.vscht.cz/veda-vyzkum/pristroje>
 36. ČSN EN ISO 10545-3 (725110) (2018). Keramické obkladové prvky – Část 3: Stanovení nasákavosti, zdánlivé pórovitosti, zdánlivé hustoty a objemové hmotnosti. Český normalizační institut.
 37. Laboratory of X-ray Diffractometry and Spectrometry. [online]: <https://clab.vscht.cz/rtg-en/equipment>
 38. Přístrojové vybavení. [online]: <https://ukmki.vscht.cz/veda-a-vyzkum/pristrojove-vybaveni#>
 39. Kloužková A., Zemenová P., Kloužek J., Pabst W. (2012). *Termická analýza, Studijní materiály 2012*. „Zřízení laboratoře pro praktickou výuku termické analýzy se zaměřením na anorganické nekovové materiály“.
 40. Blažek A. (1972). *Termická analýza*. 1st ed. Praha: SNTL.
 41. Kloužková A., Zemenová Z., Kohoutková M. (2016): Ageing of fired-clay ceramics: Comparative study of rehydroxylation processes in a kaolinitic raw material and moon-shaped ceramic idol from the Bronze Age. *Applied Clay Science*, 119(2), 358–364. doi: 10.1016/j.clay.2015.11.002
 42. Colomban P., Kırmızı B., Simsek Franci G. (2021): Cobalt and Associated Impurities in Blue (and Green) Glass, Glaze and Enamel: Relationships between Raw Materials, Processing, Composition, Phases and International Trade. *Minerals*, 11(6), 1–42. doi: 10.3390/min11060633
 43. Fanderlík I. (2009). *Barvení skla*. 1st ed. Práh. ISBN 978-80-7252-258-3.
 44. Gratuze B., Pactat I., Schibille N. (2018): Changes in the signature of cobalt colorants in Late Antique and Early Islamic glass production. *Minerals*, 8(225), 1–20. doi: 10.3390/min8060225
 45. Zlámalová Cílová Z., Gelnar M., Randáková S. (2020): Smalt production in the ore mountains: characterization of samples related to the production of blue pigment in Bohemia. *Archaeometry*, 40(2), 241–260. doi: 10.1111/arc.12584
 46. Drahotová O. (2005). *Historie sklářské výroby v českých zemích I díl. Od počátku do konce 19. století*. Academia, 138, 402-404. ISBN 80-200-1287-7.
 47. Coutinho M.L., Miller A.Z., Macedo M.F. (2015): Biological colonization and biodeterioration of architectural ceramic materials: An overview. *Journal of Cultural Heritage*, 16(5), 759–777. doi: 10.1016/j.culher.2015.01.006
 48. Moorehead D.R. (1986): Cementation by the carbonation of hydrated lime. *Cement and Concrete Research*, 16, 700–708. doi: 10.1016/0008-8846(86)90044-X